

Precursor-Mediated Crystallization Process in Suspensions of Hard Spheres

T. Schilling

Theory of Soft Condensed Matter, University of Luxembourg, Luxembourg, Luxembourg

H. J. Schöpe and M. Oettel

Institut für Physik, Universität Mainz, Mainz, Germany

G. Opletal and I. Snook

School of Applied Sciences, RMIT University, Melbourne, Australia

(Received 11 March 2010; revised manuscript received 15 April 2010; published 8 July 2010)

We report on a large scale computer simulation study of crystal nucleation in hard spheres. Through a combined analysis of real- and reciprocal-space data, a picture of a two-step crystallization process is supported: First, dense, amorphous clusters form which then act as precursors for the nucleation of well-ordered crystallites. This kind of crystallization process has been previously observed in systems that interact via potentials that have an attractive as well as a repulsive part, most prominently in protein solutions. In this context the effect has been attributed to the presence of metastable fluid-fluid demixing. Our simulations, however, show that a purely repulsive system (that has no metastable fluid-fluid coexistence) crystallizes via the same mechanism.

DOI: [10.1103/PhysRevLett.105.025701](https://doi.org/10.1103/PhysRevLett.105.025701)

PACS numbers: 64.70.dg, 47.57.J-, 61.20.Ja, 82.70.Dd

The crystallization process in complex fluids is not trivial. For systems such as solutions of proteins, alkanes, and colloids it has been shown that crystal nucleation rates can be enhanced considerably if the supersaturated liquid is quenched to a state that lies close to a metastable fluid-fluid critical point [1–8]. The enhanced nucleation rate is generally attributed to the fact that the density fluctuations occurring in the vicinity of a metastable fluid-fluid critical point enable the system to evolve via a two-step process. First, dense, amorphous precursors form and then the crystallization process takes place inside these. The prerequisite of this process scenario, the metastable fluid-fluid critical point, is easily realized in the systems listed above, which exhibit an interplay of repulsive and attractive interactions.

However, it is worthwhile asking whether the two-step process occurs more generally. Surprisingly, there have been experiments indicating two-step crystallization occurring also in hard sphere systems, the simplest model system for liquids and crystals (see, e.g., Ref. [9]). As the interaction energy between two hard spheres is either zero (no overlap) or infinite (overlap), the phase behavior of the system is purely determined by entropy. In particular, for one component hard spheres there exists a stable crystalline phase but no metastable fluid-fluid demixing region.

The crystallization kinetics in colloidal hard sphere systems has been studied experimentally using predominantly time resolved light scattering [9–15] and to a lesser extend real-space imaging techniques [16–19]. In the scattering experiments described in Refs. [9,15,20], the time evolution of the structure factor has been interpreted using a two-step process model: In the induction stage precursors (compressed, structurally heterogeneous clusters) slowly

grow. Then the precursors are converted into highly ordered crystals in a fast, activated process. In Ref. [9] it was suggested that size polydispersity limited growth is responsible for the induction stage. However, later it was argued that the precursor stage behaves in a similar fashion, regardless of polydispersity or of metastability, suggesting that the precursor nucleation and the following conversion is not a special feature of polydisperse samples, but that it might constitute a fundamental process of crystal nucleation [15].

The complete mechanism of precursor to crystal conversion is still unknown and difficult to obtain via structure factor analysis alone. A real-space experiment would be highly desired. But as size polydispersity cannot be avoided in a lab experiment, a high precision computer study appears to be the best choice.

Hard spheres are easily realized on the computer. Simulations of hard sphere crystallization have been reported, e.g., in Refs. [21–23] and of crystal nucleation kinetics, e.g., in Refs. [24,25]. One should bear in mind, however, that nucleation is a typical example of a rare event, i.e., an event that has a low reaction rate but high impact on the properties of a system. Rare events, and, in particular, nucleation, are very often simulated by methods that are based on transition state theory [26]. The basic assumption underlying transition state theory is that the rare process can be reduced to the dynamics of “slow” variables which evolve in an effective free energy landscape formed by the “fast” variables (i.e., those that quickly adopt a Boltzmann distribution). The choice of slow variables already presupposes a certain dynamic scenario which does not necessarily hold in the experimental system. For instance, the transition rates computed in [25]

using transition state theory correspond to a one-step crystallization process and the results are in disagreement with the experimental results. Therefore we have carried out a computer simulation study which follows the nucleation kinetics directly (without using any biasing scheme that would require underlying assumptions on the nucleation pathway) and therefore allows for direct comparison to experiments.

We have performed Monte Carlo simulations of $N = 216\,000$ hard spheres in a box of volume $V = 59.2 \times 59.8 \times 59.2 D^3$, where D is the particle diameter. In the following we use the particle diameter as unit of length, $k_B T$ as unit of energy, and attempted MC moves per particle (“sweeps”) as unit of time. The system was prepared by a fast pressure quench from the stable liquid. The subsequent crystallization dynamics were simulated at fixed N , V , and T by small translational MC moves only—a method which mimics Brownian dynamics on long time scales [27,28]. We used this approach because it requires relatively little CPU time per move, a necessary property when running a simulation of such a large size. We let the system evolve for 10^6 MC sweeps and sampled observables every 5000 sweeps. The number density after the quench was $N/V = 1.03$ (volume fraction $\phi = 0.54$), a value which lies in the liquid-solid coexistence region close to the density of the solid at coexistence (ca. 9% above the coexistence density of the liquid). This corresponds to a chemical potential difference between the metastable liquid and the stable, almost completely crystalline state of $\Delta\mu \approx -0.58$. Given that the interfacial tension is of the order of 0.5 [29,30], one would expect the system to be far beyond the classical nucleation regime and to crystallize almost instantaneously. The self-diffusion constant was $D_S = 2.3 \times 10^{-5}$.

We monitored crystallization by means of the $q_6 q_6$ bond-order parameter [31–33]. For a particle i with $n(i)$ neighbors, the local orientational structure is characterized by

$$\bar{q}_{lm}(i) := \frac{1}{n(i)} \sum_{j=1}^{n(i)} Y_{lm}(\vec{r}_{ij}),$$

where $Y_{lm}(\vec{r}_{ij})$ are the spherical harmonics corresponding to the orientation of the vector \vec{r}_{ij} between particle i and its neighbor j in a given coordinate frame. As we are interested in local fcc, hcp, or rcp structures, we consider $l = 6$. We assign a vector $\vec{q}_6(i)$ to each particle, the elements $m = -6, \dots, 6$ of which are defined as

$$q_{6m}(i) := \frac{\bar{q}_{6m}(i)}{(\sum_{m=-6}^6 |\bar{q}_{6m}(i)|)^{1/2}}. \quad (1)$$

Particles are counted as neighbors if $r_{ij} < 1.4$. Two neighboring particles i and j were regarded as “bonded,” if the dot product $\vec{q}_6(i) \cdot \vec{q}_6(j)$ exceeded 0.7 (i.e., if their local orientational order added up almost coherently). $n_b(i)$ is the number of bonded neighbors of the i th particle.

Orientationally ordered clusters are defined as regions of more than two bonded particles with $n_b(i)$ exceeding some common threshold value. In particular, clusters were called “crystallites” if $n_b > 10$ (i.e., almost perfectly hexagonally ordered).

Figures 1(a) and 1(b) show system snapshots at two times. Clusters of particles with $5 < n_b < 11$ are light brown, crystallites ($n_b > 10$) are green. Figure 1(c) follows the time evolution of one crystallizing cluster. One can see that the crystallization process takes place inside a low symmetry cluster (LSC, cluster of mostly particles with $5 < n_b < 11$). To quantify this effect, Fig. 2 shows the evolution of crystallinity in more detail. In Fig. 2(a) the fractions of particles with given numbers of bonds $2 \leq n_b \leq 12$ are plotted. During an induction time of ca. 400 000 MC sweeps the amount of orientationally ordered material grows slowly. Then crystallization sets in, as shown by the evolution of particles located in pure fcc or hcp crystallites ($n_b = 12$). The growth rates of all other ordered regions are markedly smaller, in particular, for $n_b < 5$. Figure 2(b) shows the evolution of clusters with $n_b > 10$ (crystallites) and $n_b > 5$, where we distinguished between clusters that contain crystallites and clusters that do not. A particle with $5 < n_b < 11$ is not necessarily part of a LSC. It could also be located on the surface of a crystallite. To distinguish more clearly between these cases, Figs. 2(c) and 2(d) show cluster size distributions for two times. In the beginning (time 300 000 sweeps) there are many pure LSCs made of up to several dozens of particles, and a number of large LSCs containing small crystallites: during the induction stage most of the particles with $5 < n_b < 11$ are not located on the surfaces of crystallites but in LSC. During crystallization (time 600 000 sweeps) the distribution of pure LSC has hardly changed, while the clusters of

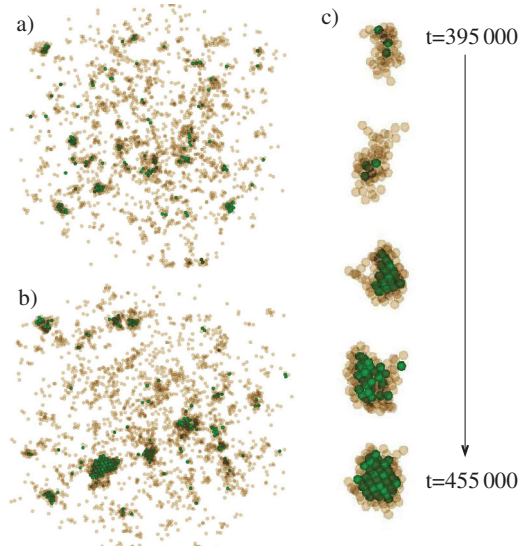


FIG. 1 (color). System snapshots at (a) 350 000 sweeps and (b) 450 000 sweeps. Particles with $n_b > 5$ (light brown) and $n_b > 10$ (green). Particles with fewer bonds are not shown. (c) Time series of cluster evolution.

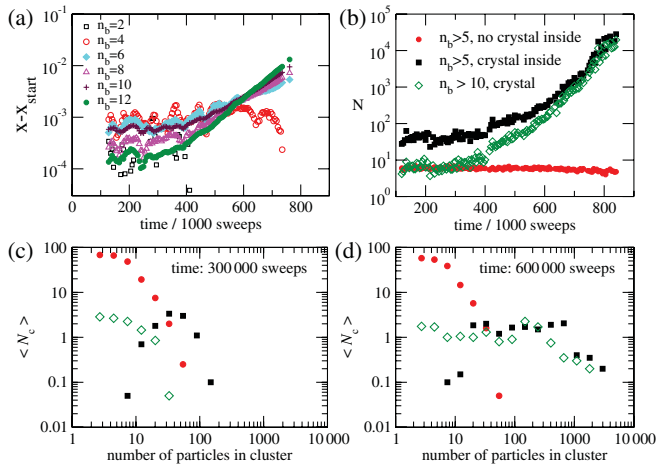


FIG. 2 (color). Evolution of crystallinity. (a) Fraction X of particles in clusters for various values of n_b [number of crystalline bonds according to Eq. (1) and text thereafter]. (b) Number of particles in crystallites (clusters with $n_b > 10$, open green diamonds) and in clusters with $n_b > 5$ either containing crystallites (black squares) or not containing crystallites (red circles). (c),(d) Cluster size distribution at $t = 300\,000$ and $600\,000$ sweeps. $\langle N_c \rangle$ denotes the average number of clusters per 5000 sweeps with an averaging time window of 100 000 sweeps. The meaning of the symbols is as in (b).

$n_b > 5$ with crystallites have roughly the same size distribution as the crystallites, indicating that particles with $5 < n_b < 11$ are now mainly surface particles.

To compare the simulation with light scattering data we extracted the radially averaged pair correlation function as function of time. By Fourier transformation the structure factor of the system was calculated. Following the procedure first proposed by Harland and co-workers [11], we obtained the time evolution of the crystalline structure factor (see Fig. 3). The simulation results are very similar to the ones obtained in experimental investigations [20]: At early times during the induction stage we observe only one broad peak close to the position of the fcc (111) peak stemming from the compressed precursor structures growing slowly in intensity while the width remains nearly constant. After about 500 000 sweeps a structure factor stemming from compressed random hexagonal closed packed (rhcp) crystals can be identified, the higher order reflections are clearly visible: the crystallites evolve from the initial precursor structures to a rhcp structure. After the conversion is complete the structure does not change significantly during the main crystallization stage, but the intensity increases rapidly (600 000 sweeps till end). The peaks become more narrow and shift to smaller q values.

From the integrated area, the width and position of individual Bragg peaks, the amount of crystallinity, the averaged domain size, and the volume fraction of the clusters or crystals can be obtained. While the amount of crystalline material and the lattice constant can be determined with high accuracy, there is a noteworthy systematic error in the averaged domain size in our data analysis,

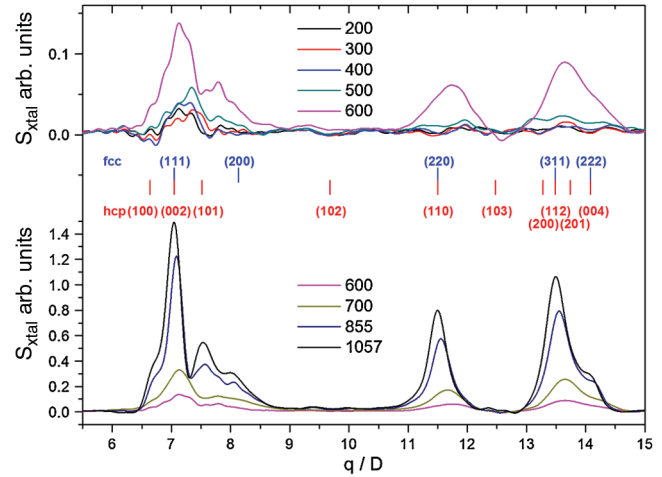


FIG. 3 (color). Evolution of crystal structure factor. Different colors correspond to different times given in 10^3 MC sweeps as indicated. For further details see text.

pertaining to Fig. 4. In a polycrystal with rhcp structure the width of the peaks is connected with the crystal size distributions of crystals with different stacking parameters [16]. In particular, the analysis of the hcp(002) [fcc(111)] reflection is difficult while the analysis of the hcp (110) [fcc(220)] peak is quite robust. As we have only a very small number of crystals in the sample, the Scherrer formula to determine the crystal size is, strictly speaking, not fulfilled due to bad statistics. Nevertheless, we show the determined quantities in Fig. 4 which can likely be compared in a qualitative way to experimental results [20].

In the induction stage the amount of orientationally ordered material and the size of the highly compressed

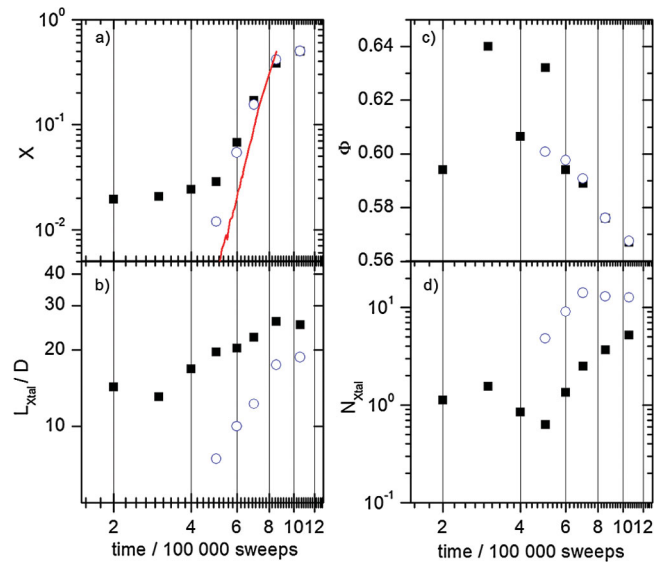


FIG. 4 (color). Evolution of parameters extracted from analysis of the crystal structure factor. (a) Crystallinity, red line: data from Fig. 2(a) ($n_b = 12$) for comparison. (b) Average domain size. (c) Volume fraction and (d) number of clusters or crystals. Black squares fcc, (111) peak; open circles, fcc (220) peak.

precursors stay nearly constant $[(2-4) \times 10^5]$ sweeps]. During conversion the precursors start growing while the increase in crystallinity is delayed and a significant drop in the number of precursors can be observed $[(3-5) \times 10^5]$ sweeps]. During the main crystallization process information stemming from the fcc(220) peak can also be obtained $[(5-11) \times 10^5]$ sweeps]. Here crystallinity increases rapidly; crystal size and the number of crystallites show their strongest increase due to crystal growth and crystal nucleation. The crystals expand to reach the equilibrium volume fraction at the end of the crystallization process (which was not reached in these calculations). As discussed above, the absolute values in the averaged crystal size stemming from the fcc(111) are prone to error leading to unphysically small values in the absolute number; however, its time trace reflects the correct trend.

We would like to emphasize that there is a remarkable resemblance of the time evolution of crystallinity extracted from the structure factor data with the crystallinity fraction extracted from the maximally bonded ($n_b = 12$) crystallites [see Fig. 4(a)]. This means that the orientation-averaged structure factor analysis can be mapped very well to the real-space analysis of the mutual particle orientations.

To summarize, we studied the nucleation process in hard spheres by combining a real-space bond-order analysis (typical for simulations and confocal microscopy experiments) with a reciprocal-space analysis of the time evolution of the structure factor (typical for scattering experiments). Our simulations showed that nucleation in hard spheres is more complex than the traditional picture of one-step classical nucleation suggests. We identified the formation of dense clusters right after the quench containing particles that have high $q_6 q_6$ coherence with at least half of their neighbors. The critical crystal nuclei observed in our simulation are not formed spontaneously in one step from random fluctuations, but they appear inside these precursors of lower symmetry. The metastable fluid relaxes the density first, by producing dense low symmetry clusters, and later crystallites of perfect structure are formed.

The two-step crystallization mechanism identified here for hard spheres is akin to processes that have been observed in protein solutions and in suspensions of attractive colloids. Thus we conclude that metastable fluid-fluid demixing is not a necessary prerequisite. Different dynamics for the two order parameters density and structure seem to suffice for a two-step nucleation process.

Financial support by SFB-TR6 and SPP1296 is gratefully acknowledged. T.S. thanks the NIC Jülich for CPU time. I. K. S. would like to thank K. Binder and T. Palberg for their hospitality when visiting Mainz.

-
- [1] L. Filobelo, O. Galkin, and P. Vekilov, *J. Chem. Phys.* **123**, 014904 (2005).
 [2] W. Pan, A. Kolomeisky, and P. Vekilov, *J. Chem. Phys.* **122**, 174905 (2005).

- [3] V. Anderson and H. Lekkerkerker, *Nature (London)* **416**, 811 (2002).
 [4] P. ten Wolde and D. Frenkel, *Science* **277**, 1975 (1997).
 [5] V. Talanquer and D. Oxtoby, *J. Chem. Phys.* **109**, 223 (1998).
 [6] A. Shiryayev and J. Gunton, *J. Chem. Phys.* **120**, 8318 (2004).
 [7] D. Kashchiev, P. Vekilov, and A. Kolomeisky, *J. Chem. Phys.* **122**, 244706 (2005).
 [8] J. Lutsko and G. Nicolis, *Phys. Rev. Lett.* **96**, 046102 (2006).
 [9] H. Schöpe, G. Bryant, and W. van Meegen, *Phys. Rev. Lett.* **96**, 175701 (2006).
 [10] K. Schtzel and B.J. Ackerson, *Phys. Rev. Lett.* **68**, 337 (1992).
 [11] J.L. Harland, S.I. Henderson, S.M. Underwood, and W. van Meegen, *Phys. Rev. Lett.* **75**, 3572 (1995).
 [12] Y. He, B.J. Ackerson, W. van Meegen, S.M. Underwood, and K. Schtzel, *Phys. Rev. E* **54**, 5286 (1996).
 [13] J.L. Harland and W. van Meegen, *Phys. Rev. E* **55**, 3054 (1997).
 [14] Z. Cheng, P. Chaikin, J. Zhu, W.B. Russel, and W. Meyer, *Phys. Rev. Lett.* **88**, 015501 (2001).
 [15] H. Schöpe, G. Bryant, and W. van Meegen, *J. Chem. Phys.* **127**, 084505 (2007).
 [16] W.K. Kegel and J.K.G. Dhont, *J. Chem. Phys.* **112**, 3431 (2000).
 [17] U. Gasser, E.R. Weeks, A. Schofield, P.N. Pusey, and D.A. Weitz, *Science* **292**, 258 (2001).
 [18] M.S. Elliot, S.B. Haddon, and W.C.K. Poon, *J. Phys. Condens. Matter* **13**, L553 (2001).
 [19] V. Prasad, D. Semwogerere, and E.R. Weeks, *J. Phys. Condens. Matter* **19**, 113102 (2007).
 [20] S. Iacopini, T. Palberg, and H. Schöpe, *J. Chem. Phys.* **130**, 084502 (2009).
 [21] T. Truskett, S. Torquato, S. Sastry, P. Debenedetti, and F. Stillinger, *Phys. Rev. E* **58**, 3083 (1998).
 [22] B. O'Malley and I. Snook, *Phys. Rev. Lett.* **90**, 085702 (2003).
 [23] B. O'Malley and I. Snook, *J. Chem. Phys.* **123**, 054511 (2005).
 [24] T. Gruhn and P. Monson, *Phys. Rev. E* **64**, 061703 (2001).
 [25] S. Auer and D. Frenkel, *Nature (London)* **409**, 1020 (2001).
 [26] H. Eyring, *J. Chem. Phys.* **3**, 107 (1935).
 [27] L. Berthier and W. Kob, *J. Phys. Condens. Matter* **19**, 205130 (2007).
 [28] Y.-H. Chui, S. Sengupta, I. Snook, and K. Binder, *J. Chem. Phys.* **132**, 074701 (2010).
 [29] R.L. Davidchack and B.B. Laird, *Phys. Rev. Lett.* **85**, 4751 (2000).
 [30] R.L. Davidchack, J.R. Morris, and B.B. Laird, *J. Chem. Phys.* **125**, 094710 (2006).
 [31] P.J. Steinhardt, D.R. Nelson, and M. Ronchetti, *Phys. Rev. B* **28**, 784 (1983).
 [32] P.R. ten Wolde, M.J. Ruiz-Montero, and D. Frenkel, *Phys. Rev. Lett.* **75**, 2714 (1995).
 [33] D. Rintoul and S. Torquato, *Phys. Rev. Lett.* **77**, 4198 (1996).